COBEM 99
XV Congresso Brasileiro de Engenharia Mecânica
15th Brazilian Congress of Mechanical Engineering
22 - 26 de Novembro de 1999 / November 22 - 26, 1999 Águas de Lindóia, São Paulo,

EFFECTS OF STRENGTH MISMATCH ON FRACTURE BEHAVIOR OF WELDED STRUCTURES

Luis R. B. Robles
Claudio Ruggieri
Department of Naval Architecture and Ocean Engineering, University of São Paulo
São Paulo, SP 05508–900, E-mail: cruggi@usp.br, Brazil

Abstract *– This study extends the Weibull stress approach to address effects of weld strength mismatch on macroscopic fracture toughness of weldments. Our approach builds on the Beremin model to establish a relationship between the microregime of fracture and macroscopic crack driving forces for bimaterial media by adopting the Weibull stress (σ_w) as a probabilistic fracture parameter. Plane-strain, small scale yielding (SSY) reference fields for stationary interface cracks are presented to provide a measure of mismatch effects. The analyses show the strong effect of the mismatch level on the magnitude of near-tip stress fields which quantifies the level of constraint (associated with strength mismatch) over distances of a few CTODs ahead of crack tip. Computation of the Weibull stress for these small scale yielding analyses under varying levels of strength mismatch provide valuable insight about the effects of weld strength mismatch on fracture resistance. Our SSY results exhibit the essential features of the micromechanics approach in correlating macroscopic fracture toughness with strength mismatch variations.*

Key words: *cleavage fracture, weldments, strength mismatch, statistical effects, local approach, Weibull stress*

1. INTRODUCTION

Brittle fracture of steel weldments (weld metal and heat affected zone - HAZ) remains a key issue for the safety assessment of critical welded structures, including offshore and pipeline facilities. Experimental and *in situ* observations consistently reveal the occurrence of crack-like defects in the welded region which are either planar (e.g., hot or cold cracking, lack of penetration, undercut) or volumetric (e.g., porosity and entrapped slag). To address the potential deleterious effects of such defects on the structural integrity, many codes and current fabrication practices require the use of weldments with weld metal strength *higher* than the base metal strength; a condition referred to as *overmatching*. Overmatch welds generally cause large plastic deformation into the lower strength base plate which (presumably) increases the load carrying capacity of the welded joint.

However, experimental investigations (see, e.g., [1-4] for illustrative data) demonstrate that overmatched welds, while used effectively in lower strength grade steels, may actually have a detrimental effect on the fracture behavior of high strength low alloy (HLSA) steels. For these materials, fracture testing of specimens with a crack located well inside the HAZ region consistently reveals low toughness values (J_c or CTOD). The overmatching condition magnifies the impact of embrittled microstructures in the HAZ region which contributes to increase the propensity to trigger cleavage before gross yield section of the structure. Realistic procedures for defect assessments must include the complex interplay between the effects of weld strength mismatch and the variability of cleavage resistance at the microstructural level for the different regions of steel weldments.

This study extends the Weibull stress approach presented in previous investigations [5-7] to address effects of weld strength mismatch on macroscopic fracture toughness of weldments. Our approach builds on the Beremin model [8,9] to establish a relationship between the microregime of fracture and macroscopic crack driving forces (such as the J–integral) for bimaterial media by adopting the Weibull stress (σ_w) as a probabilistic fracture parameter. Plane-strain, small scale yielding (SSY) reference fields for stationary interface cracks are presented to provide a measure of mismatch effects. The analyses show the strong effect of the mismatch level on the magnitude of near-tip stress fields which quantifies the level of constraint (associated with strength mismatch) over distances of a few CTODs ahead of crack tip. Computation of the Weibull stress for these small scale yielding analyses under varying levels of strength mismatch provide valuable insight about the effects of weld strength mismatch on fracture resistance. Our SSY results exhibit the essential features of the micromechanics approach in correlating macroscopic fracture toughness with strength mismatch variations.

2. THE WEIBULL STRESS FOR BIMATERIAL SYSTEMS

The Weibull stress (σ_w) [8,9] was derived in previous work [5-7] as a probabilistic fracture parameter to provide a robust coupling between the microregime of fracture (which includes a local failure criterion *and* the stresses that develop ahead of a macroscopic crack) with macroscopic (remote) loading (such as the J integral). For a stationary macroscopic crack lying in homogeneous materials, the Wribull stress is given by integration of the (local) principal stress over the fracture process zone in the form [10-14]

$$\sigma_w = \left[\frac{1}{V_0} \int_{\Omega} {\sigma_1}^m d\Omega \right]^{1/m} , \tag{1}$$

where σ_1 is the maximum principal stress, Ω denotes the volume of the (near-tip) fracture process zone defined by the loci $\sigma_1 \geq \lambda\sigma_0$ with $\lambda \approx 2$, and parameter m (the Weibull modulus) define the microcrack distribution.

For bimaterial systems, such as the interfacial crack along the boundary between the weld metal and the base plate schematically represented in Fig. 1, the fracture process may result from a complex interplay of the operative failure mechanism for each individual material. For a given remote loading, the *mismatch* in mechanical properties, such as E/σ_0 and ν, between both materials produce crack-tip stress and strain fields quite different than the fields that arise in corresponding homogeneous material. Moreover, with increased levels of strength mismatch between both media, the fracture process zone for each material differ significantly from those of a homogeneous material.

In the present work, we adopt a simplified form for σ_w applicable to bimaterial systems. Referring to Fig. 1 which shows a crack lying along an interface separating material 1 and mateial 2, we define the Weibull stress corresponding to each media as

$$\sigma_w^k = \left[\frac{1}{V_0} \int_{\Omega_k} {\sigma_1}^{m_k} d\Omega_k \right]^{1/m_k} , \tag{2}$$

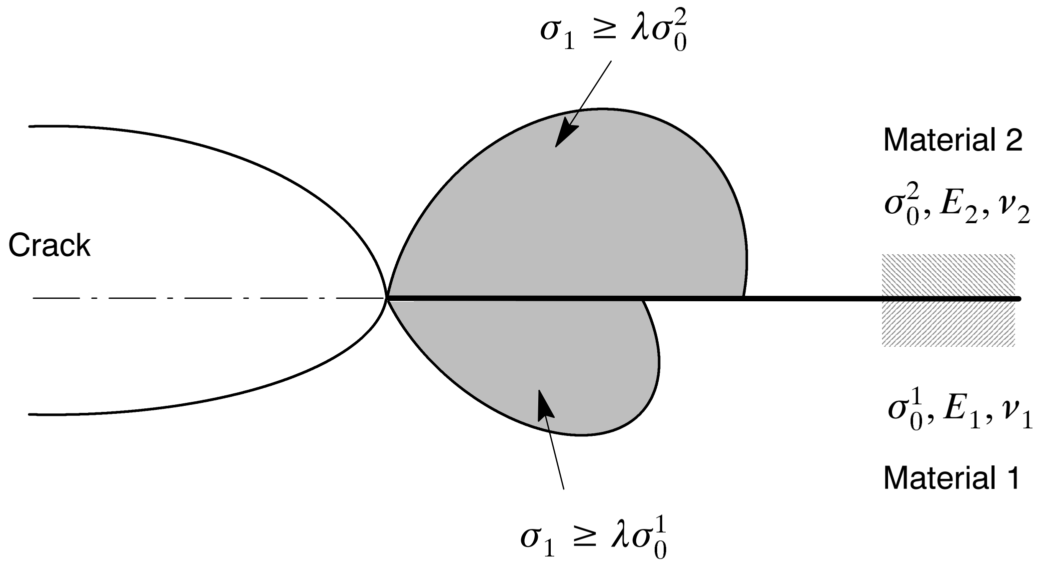

Fig. 1. Schematic representation for an interface (macroscopic) crack in a bimaterial system.

where the subscript k denotes the *k-th* material, Ω_k is the fracture process zone for material k and m_k denotes the Weibull modulus for material k. Since the Weibull stress can be associated with a crack-tip driving force incorporating a local failure criterion (see Ruggieri and Dodds [10-14]), the present definition for σ_w implies that fracture of the entire bimaterial system takes place in *only one* material, i.e., only one material controls failure. As demonstrated by extensive experimental work of Toyoda and co-workes (see [1-4] for illustrative data), such definition is sufficiently realistic when assessing the fracture behavior of HSLA steel weldments while, at the same time, providing valuable insight about effects of weld strength mismatch on fracture resistance of weldments.

3. COMPUTATIONAL PROCEDURES AND FINITE ELEMENT MODELS

3.1 Small Scale Yielding Model

The modified boundary layer model (MBL) [17] simplifies the generation of numerical solutions for stationary interface cracks under well-defined SSY conditions with varying levels of strength mismatch. Figure 2 shows the plane-strain finite element model for an infinite domain, single-ended interface crack with an initially blunted notch (finite root radius, $\rho = 10\mu$m). The SSY model has one thickness layer of 4130 8-node, 3-D elements with plane-strain constraints imposed on all nodes.

With the plastic region limited to a small fraction of the domain radius, $R_p < R/20$ (R is the radius of the outer circular boundary), the general form of the asymptotic crack-tip stress fields well outside the plastic region is given by [16]

$$\sigma_{ij} = \frac{K_\mathrm{I}}{\sqrt{2\pi r}} f_{ij}(\theta) + T\delta_{1i}\delta_{1j} \tag{3}$$

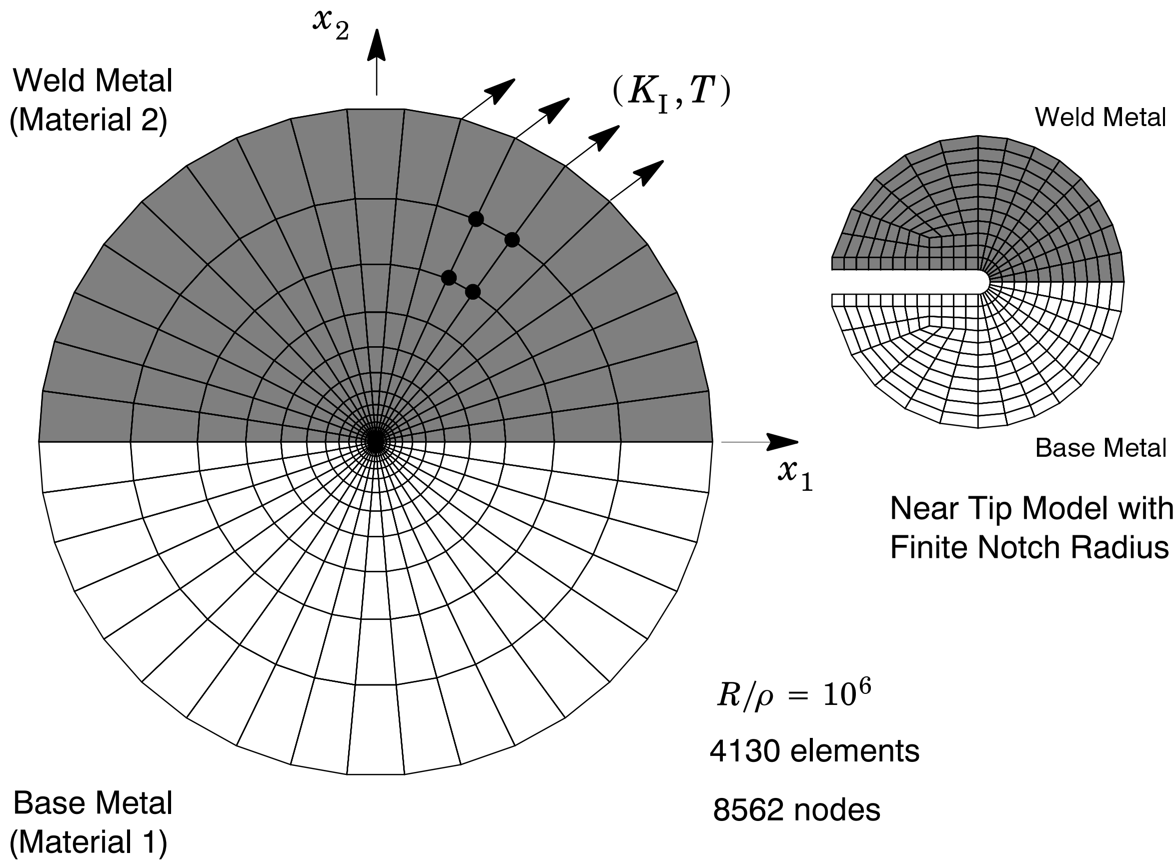

Fig. 2. SSY model for an interface crack with (K, T) fields imposed on boundary.

where K is the stress intensity factor, $f_{ij}(\theta)$ define the angular variations of in-plane stress components, and the non-singular term T represents a tension (or compression) stress parallel to the crack. In the present investigation, numerical solutions for $T = 0$ are generated by imposing displacements of the elastic, Mode I singular field on the outer circular boundary ($r = R$) which encloses the crack

$$u(R,\theta) = K_I \frac{1+\nu}{E}\sqrt{\frac{R}{2\pi}}\cos\left(\frac{\theta}{2}\right)(3 - 4\nu - \cos\theta) \tag{4}$$

$$v(R,\theta) = K_I \frac{1+\nu}{E}\sqrt{\frac{R}{2\pi}}\sin\left(\frac{\theta}{2}\right)(3 - 4\nu - \cos\theta)) \tag{5}$$

3.2. Constitutive Models

The elastic-plastic material employed in the analyses follows a J_2 flow theory with conventional Mises plasticity. The uniaxial true stress-logarithmic strain curve obeys a simple power-hardening model in the form

$$\frac{\epsilon}{\epsilon_0} = \frac{\bar{\sigma}}{\sigma_0} \quad \epsilon \le \epsilon_0 \ ; \qquad \frac{\epsilon}{\epsilon_0} = \left(\frac{\bar{\sigma}}{\sigma_0}\right)^n \quad \epsilon > \epsilon_0 \tag{6}$$

where σ_0 and ϵ_0 are the reference (yield) stress and strain, and n is the strain hardening exponent.

The finite element analyses consider material flow properties for the base metal (material 1) representing a typical structural steel with $n = 10$ (moderate hardening) and $E/\sigma_0 = 500$.

From these mechanical properties for the base metal, the matrix analysis for the weld / base metal system is constructed by adopting the flow properties for the weld metal (material 2) as shown on Table 1.

Table 1 Mechanical properties for the bimaterial system employed in the analyses.

	σ_0^1 (MPa)	n^1	σ_0^2 (MPa)	n^2
0.8 Undermatch	412	10	330	5.9
Evenmatch	412	10	412	10
1.2 Overmatch	412	10	495	13.5
1.5 Overmatch	412	10	618	18

The ranges of properties presented on Table 1 reflect the upward trend in yield stress with the decrease in strain hardening exponent characteristic of ferritic steels. In all analyses, $E = 206$ GPa and $\nu = 0.3$.

3.3. Finite Element Procedures

The three-dimensional computations reported here are generated using the research code WARP3D [15] which: (1) implements a Mises constitutive models in a finite-strain framework, (2) solves the equilibrium equations at each iteration using a linear pre-conditioned conjugate gradient (LPCG) method implemented within an element-by-element (EBE) software architecture, (3) evaluates the J-integral using a convenient domain integral procedure and (4) analyzes fracture models constructed with three-dimensional, 8-node tri-linear hexahedral elements.

Evaluation of the Weibull stress requires integration over the process zone, including the region as $r \to 0$. The SSY and all other crack models previously described have a small initial root radius at the crack front (blunt tip) which provides two numerical benefits: (1) it accelerates convergence of the finite-strain plasticity algorithms during the initial stage of blunting, and (2) it minimizes numerical problems during computation of the Weibull stress over material incident on the crack tip.

4. EFFECT OF STRENGTH MISMATCH ON CRACK-TIP STRESS FIELDS

Figures 3 and 4 provide key results to assess effects of weld strength mismatch on the crack-tip stress fields for the bimaterial system employed in the analyses. Figures 3(a-d) shows the near-tip stress distribution (opening stress) in the *base metal side* under increasing deformation for all levels of strength mismatch. Similarly, Figs. 4(a-d) shows the near-tip stress distribution (opening stress) in the *weld metal side* under increasing deformation for all levels of strength mismatch. In these plots, the normalizing stress corresponds to the yield stress for material upon which the opening stresses are computed, i.e., distances all scale with $(K_I/\sigma_0^k)^2$ whereas the opening stresses are normalized by σ_0^k with $k = 1, 2$.

At very low remote loading for all levels strength mismatch ($K_I = 10 \sim 40\text{MPa}\sqrt{\text{m}}$), the near-tip stresses increase as the process of crack-tip blunting takes place. After the notch root radius increases to several times the initial radius ρ, a *steady state solution* develops so that the near-tip fields under SSY conditions are simply a continuous series of self-similar states. These plane-strain fields thus define a family of reference fields for stationary cracks where specified values for K_I uniquely define the elastic-plastic fields along the crack tip when a vanishingly small plastic zone encloses the tip.

The central feature of the results displayed in those plots is the strong effect of strength mismatch on the magnitude of the near-tip opening stresses. Compared to the homogeneous case (evenmatched material system – see Figs. 3(a) and 4(a)), strength overmatching produces a significant increase of the near-tip opening stresses in the base metal side whereas strength undermatching causes an increase of the near-tip opening stresses in the weld metal side – see Fig. 3(d). These trends are consistent with previous numerical analyses in that strength mismatch alter significantly the crack-tip stress fields for an interface crack when compared with those for a crack in a homogeneous material [18]. In summary, these representative analyses clearly demonstrate that strength mismatch between the weld metal and base plate promotes an increase in the magnitude of the stresses that develop ahead of a (macroscopic) interface crack for the *weaker* material.

5. EFFECT OF STRENGTH MISMATCH ON FRACTURE RESISTANCE

The simplified form of the Weibull stress, given by Eq. (2), provides the basis to assess effects of strength mismatch on the fracture resistance for bimaterial systems, such as the one depicted in Fig. 2. The procedure relies on the notion of σ_w as the crack-tip driving force [10-14] which establishes a robust coupling between the applied load and level of mismatch thereby describing the local, crack-tip response for cleavage fracture.

Figure 5 displays the evolution of the Weibull stress normalized by the yield stress σ_0^k ($k = 1$, 2) (note that the normalizing stress corresponds to the material upon which σ_w is computed) with increased loading. For all levels of mismatch and material combination, the Weibull stress increases monotonically with the K-levels. The most striking feture of these results is the development of σ_w with increasing loading for the mismatched conditions (see Figs. 5(b-d). The *normalized* levels of σ_w for the *weaker* material are consistently higher than the corresponding σ_w-levels for the stronger material in all material combinations. In the context of the micromechanics approach adopted in the present work, such results provide important features associated with the fracture resistance of weldments (and general bimaterial systems as well). The physical significance is this: strength overmatch and strength undermatch promotes reduction in the fracture resistance for the base metal side. In particular, the effect of strength overmatch on the fracture resistance of weldments has important implications for the fracture behavior of HAZ-notched welded joints. Weld overmatch, while “shielding” the weld metal region, causes substantial increase in the crack-tip driving force for the HAZ region (as quantified by σ_w). Because this region may contain a large amount of brittle constituents (which exhibit very low fracture resistance), the load-carrying capacity of the welded joint may be significantly reduced.

6. CONCLUDING REMARKS

We have presented a micromechanics-based framework to assess the effects of strength mismatch on fracture resistance of weldments which has strong implication on macroscopic measures of cleavage fracture toughness (J_c, δ_c) for welded joints and welded components. To incorporate the pronounced effects of strength mismatch on the crack-tip stress fields and on the near-tip stressed volume (i.e., the fracture process zone ahead of the crack) we employ the Weibull stress, σ_w, as a near-tip, or *local,* fracture parameter. The strength mismatch affects the

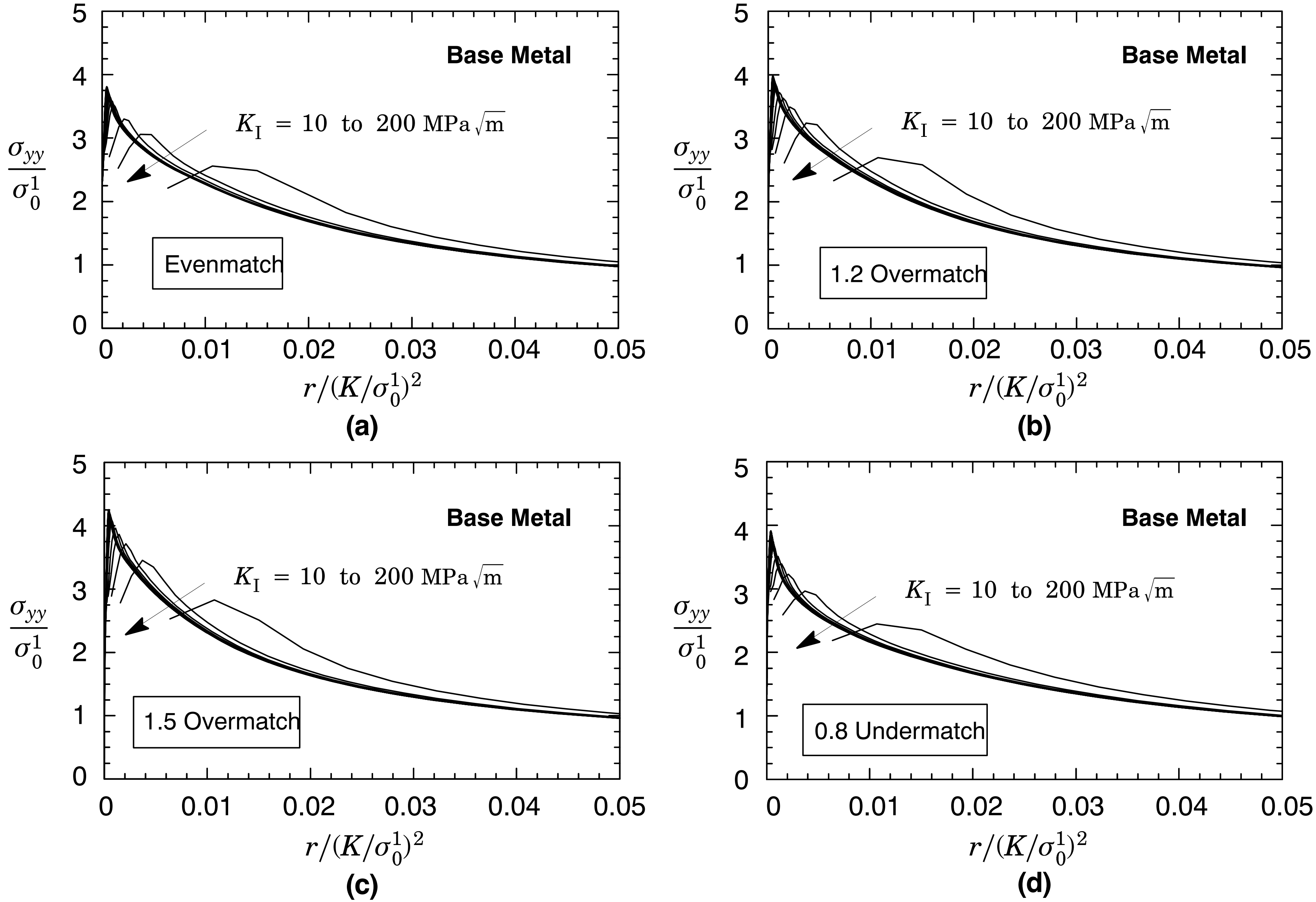

Fig. 3. Near-tip opening stresses under SSY conditions in the base metal side varying levels of strength mismatch. Plots are generated for load levels $K_I = 10$ to 200 MPam$^{1/2}$ with increments of 10 MPam$^{1/2}$.

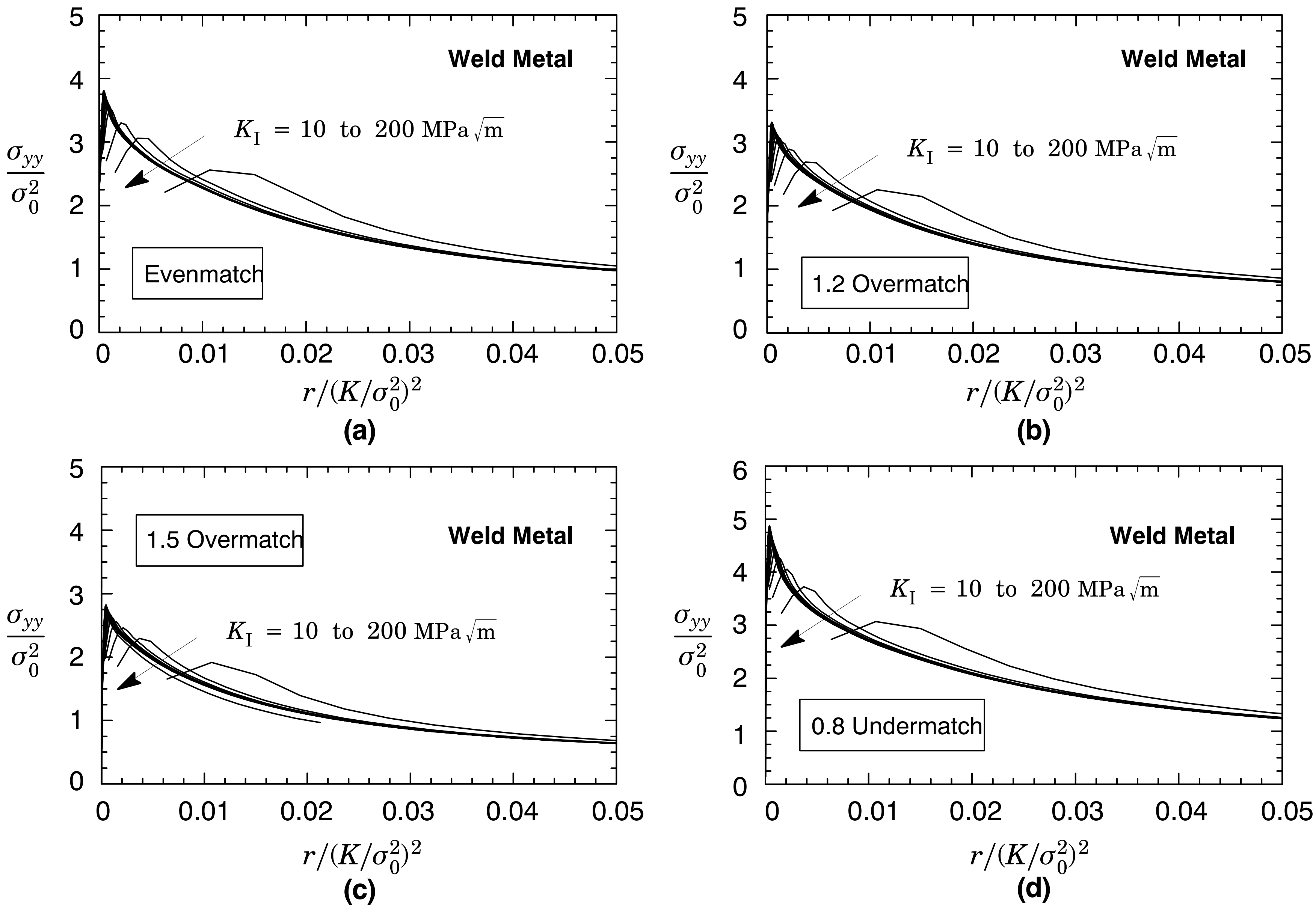

Fig. 4. Near-tip opening stresses under SSY conditions in the weld metal side varying levels of strength mismatch. Plots are generated for load levels $K_I = 10$ to 200 MPam$^{1/2}$ with increments of 10 MPam$^{1/2}$.

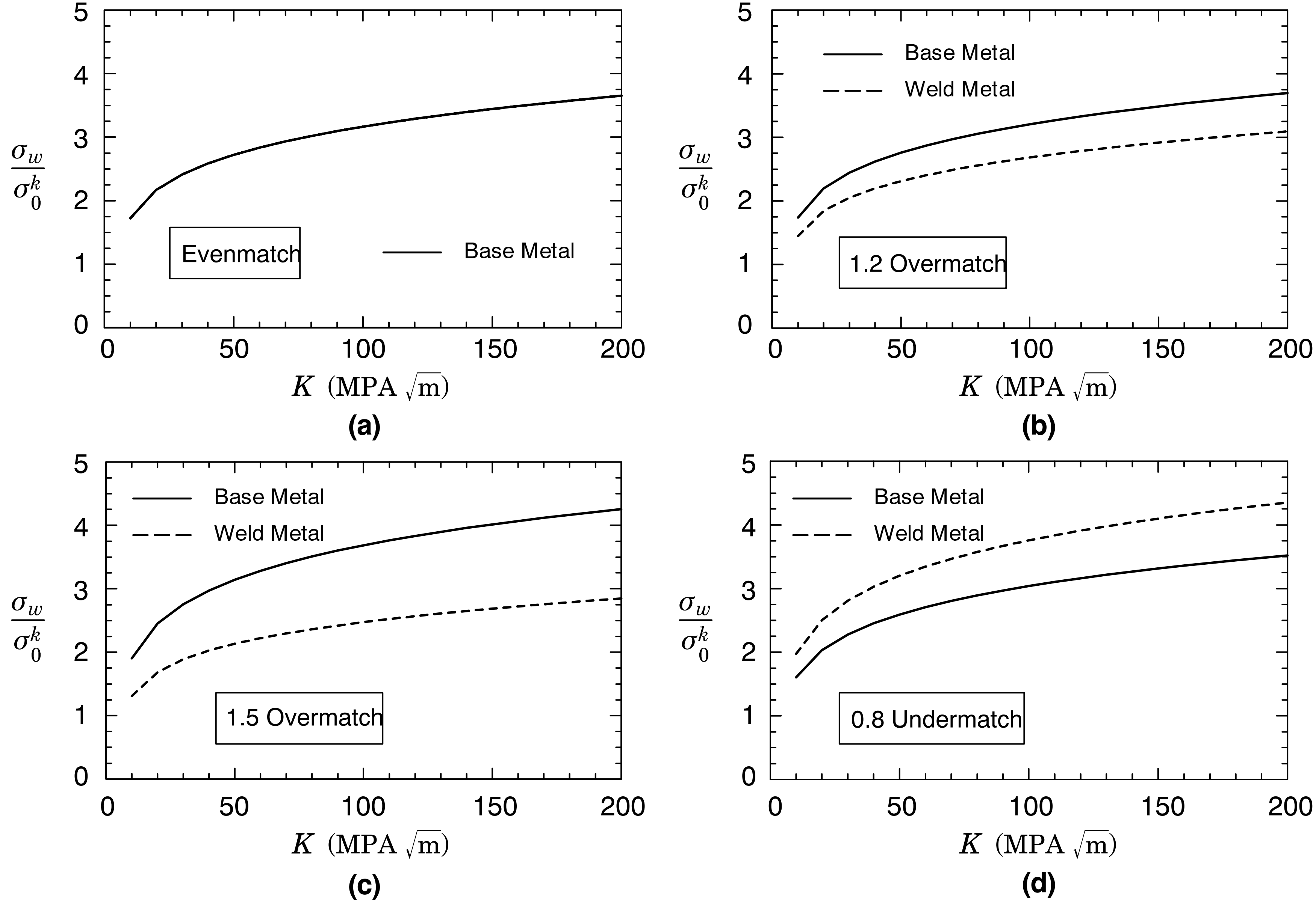

Fig. 5. Weibull stress trajectories for the SSSY model with varying levels of mismatch.

evolution of σ_w under increasing applied load which reflects on fracture resistance of weldments. Our representative analyses have clearly demonstrated that strength mismatch between the weld metal and base plate promotes an increase in the magnitude of the stresses that develop ahead of a (macroscopic) interface crack for the *weaker* material. Consequently, weld overmatch may reduce substantially the load-carrying capacity of HAZ-notched welded joints with weld metal overmatch. While we have not explored an extensive range of material combinations, the relative operational simplicity and robustness of the Weibull stress approach encourages further investigations in procedures for fracture assessments of welded structures. Further work is in progress to develop a more refined framework employing the Weibull stress more applicable to bimaterial and trimaterial systems.

Acknowledgements

This investigation was supported by grants principally from the Scientific Foundation of the State of São Paulo (FAPESP) under Grant 98/10574-2. Access to the SGI-Origin 200 at the High Performance Computing Center (LCCA) of the University of São Paulo is gratefully acknowledged.

References

1. Minami, F., Toyoda, M. and Ruggieri, C. , "Significance of Shallow Notch CTOD Test in Fracture Performance Evaluation of Welded Joint," in *Offshore Mechanics and Artic Engineering Conference (OMAE)*, Vol.III-B, pp. 761-768, 1993, Glasgow.
2. Webster, S. E. and Walker, E. F.. , "The Significance of Local Brittle Zones to the Integrity of Large Welded Structures," in *Offshore Mechanics and Artic Engineering Conference (OMAE)*, 1988, Houston.
3. Suzuki, S., Bessyo, K., Toyoda, M. and Minami, F.. , "Property Distribution Map to Understand HAZ CTOD Toughness," in *Offshore Mechanics and Artic Engineering Conference (OMAE)*, Vol.III-B, pp. 753-760, 1993, Glasgow.
4. Thaulow, C., Paauw, A. J., Hauge, M., Toyoda, M and Minami. , "Fracture Property of HAZ-Notched Weld Joint with Mechanical Mismatching," in *Symposium of Mis-Matching of Welds* (Eds. Schwalbe and Koçak), pp. 417-432, 1994.
5. Ruggieri, C., "A Framework to Correlate Effects of Constraint Loss and Ductile Tearing on Fracture Toughness – Part I: Probabilistic Approach," *15^{th} Brazilian Congress of Mechanical Engineering (Cobem 99)*, Águas de Lindóia, Brazil (1999).
6. Ruggieri, C. and Trovato, E, "A Framework to Correlate Effects of Constraint Loss and Ductile Tearing on Fracture Toughness – Part II: Fracture Under Small Scale Yielding Conditions," *15^{th} Brazilian Congress of Mechanical Engineering (Cobem 99)*, Águas de Lindóia, Brazil (1999).
7. Ruggieri, C., "A Framework to Correlate Effects of Constraint Loss and Ductile Tearing on Fracture Toughness – Part III: Parameter Calibration and Fracture Testing," *15^{th} Brazilian Congress of Mechanical Engineering (Cobem 99)*, Águas de Lindóia, Brazil (1999).
8. Beremin, F.M, "A Local Criterion for Cleavage Fracture of a Nuclear Pressure Vessel Steel," *Metallurgical Transactions,* Vol. 14A, pp. 2277–2287, 1983.
9. Mudry, F., 1987, "A Local Approach to Cleavage Fracture", *Nuclear Engineering and Design*, Vol. 105, pp. 65–76.
10. Ruggieri, C. and Dodds, R. H., "A Transferability Model for Brittle Fracture Including Constraint and Ductile Tearing Effects: A Probabilistic Approach," *International Journal of Fracture*, Vol. 79, pp. 309-340, 1996.
11. Ruggieri, C. and Dodds, R. H., "Probabilistic Modeling of Brittle Fracture Including 3-D Effects on Constraint Loss and Ductile Tearing," *Journal de Physique*, Vol. 1996.
12. Ruggieri, C. and Dodds, R. H., "WSTRESS Release 1.0: Numerical Computation of Probabilistic Fracture Parameters for 3-D Cracked Solids," *BT–PNV–30 (Technical Report)*, EPUSP, University of São Paulo, 1997.
13. Ruggieri, C. and Dodds, R. H., "Numerical Computation of Probabilistic Fracture Parameters Using WSTRESS," *Engineering Computations*, Vol. 15, pp. 49-73, 1998.
14. Ruggieri, C., Dodds, R. H. and Wallin, K., "Constraints Effects on Reference Temperature, T_0, for Ferritic Steels in the Transition Region," *Engineering Fracture Mechanics*, Vol. 60, pp. 19-36, 1998.
15. Koppenhoefer, K., Gullerud, A., Ruggieri, C., Dodds, R. and Healy, B., "WARP3D: Dynamic Nonlinear Analysis of Solids Using a Preconditioned Conjugate Gradient Software Architecture", *Structural Research Series (SRS) 596*, UILU–ENG–94–2017, University of Illinois at Urbana–Champaign, 1994.
16. Williams, M.L., "On the Stress Distribution at the Base of a Stationary Crack", *Journal of Applied Mechanics,* Vol. 24, pp. 109–114, 1957.
17. Larsson, S. G. and Carlsson, A. J., "Influence of Non–Singular Stress Terms and Specimen Geometry on Small Scale Yielding at Crack–Tips in Elastic–Plastic Materials", *Journal of the Mechanics and Physics of Solids*, Vol. 21, pp. 447–473, 1973.
18. Ruggieri, C., Minami, F. and Toyoda, M, "Effect of Weld Strength Mismatch in HAZ-Notched Welded Joints Subjected to Bending and Tension," *Journal of the Society of Naval Architects of Japan*, Vol. 174, pp. 543–549, 1993.